5-2010

Development of hydrogen direct injection for conversion of internal combustion engines

Maxwell A. Wilson
University of Nevada Las Vegas

DEVELOPMENT OF HYDROGEN DIRECT INJECTION FOR CONVERSION OF INTERNAL COMBUSTION ENGINES

by

Maxwell A. Wilson

Bachelor of Science, Chemistry
University of Nevada, Las Vegas
2002

A thesis submitted in partial fulfillment
of the requirements for the

Master of Science in Mechanical Engineering
Department of Mechanical Engineering
Howard R. Hughes College of Engineering

Graduate College
University of Nevada Las Vegas
May 2010

UNIVERSITY OF NEVADA LAS VEGAS

THE GRADUATE COLLEGE

We recommend the thesis prepared under our supervision by

Maxwell A. Wilson

entitled

Development of Hydrogen Direct Injection for Conversion of Internal Combustion Engines

be accepted in partial fulfillment of the requirements for the degree of

Master of Science in Mechanical Engineering

Robert Boehm, Ph.D., Committee Chair

Yitung Chen, Ph.D., Committee Member

Suresh Sadineni, Ph.D., Committee Member

Yahia Baghzouz, Ph.D., Graduate Faculty Representative

Ronald Smith, Ph. D., Vice President for Research and Graduate Studies
and Dean of the Graduate College

May 2010

ABSTRACT

Development of Hydrogen Direct Injection for Conversion of Internal Combustion Engines

by

Maxwell A. Wilson

Dr. Robert Boehm, Examination Committee Chair
Distinguished Professor of Mechanical Engineering
University of Nevada, Las Vegas

The trend toward usage of vehicles that operate on alternative, renewable forms of energy storage has generated areas for development of new products that will facilitate implementation of new automotive fuel systems. As the reality of a hydrogen-fueled economy emerges, intermediate technologies may be necessary for the transition between hydrocarbon fueled internal combustion engines and hydrogen powered fuel cells. The UNLV Center for Energy Research (CER) has developed a method for converting the common hydrocarbon fueled internal combustion engine to hydrogen direct injected fueling. This thesis describes the second phase of development and involves the design, fabrication and characterization of a spark plug/fuel injector assembly which will allow conversion to hydrogen direct injection fueling without disassembly/modification of internal engine components. Characterization of these assemblies includes response time testing of the solenoids used and flow rate testing of the assemblies at various pressures and operational frequencies.

TABLE OF CONTENTS

LIST OF TABLES

LIST OF FIGURES

NOMENCLATURE

AFR	air fuel ratio
ATV	all terrain vehicle
BTDC	before top dead center
CER	UNLV Center for Energy Research
CNG	compressed natural gas
COV	combustion cycle coefficient of variation
DI	direct injection
duty cycle	percentage of time of operation to time available
ECM	engine control module
F	force
FAR	fuel air ratio
GM	General Motors
HC	hydrocarbon
HICE	hydrogen internal combustion engine
Hz	frequency units (s^{-1})
LVVWD	Las Vegas Valley Water District
MAP	manifold absolute pressure
MBT	mean best torque
PCM	powertrain control module
PT	pressure transducer
Rpm	revolutions per minute
T	temperature sensor
TDC	top dead center
TDC	top dead center
TIG	tungsten inert gas
V	volume
W	weight
ρ	density
λ	lambda, ratio of observed AFR to stoichiometric AFR
Φ	phi, equivalence ratio, ratio of observed FAR to stoichiometric FAI

CHAPTER 1

INTRODUCTION

The internal combustion engine powered automobile has been in use for well over a century and though vast improvements have been made to its various systems one constant has remained the same for the majority of autos. The form of energy used to propel them consists of various hydrocarbon fuels, most commonly gasoline and diesel. The simple reason for this is oil has been an inexpensive, easily accessible and plentiful resource. Gasoline has relatively high energy density by both volume and mass at roughly 940,000 Btu/ft^3 and 20,000 Btu/lb, respectively which make it a near perfect candidate for this application [1]. Unfortunately, with the increase in hydrocarbon fuel demand, its finite supply along with the economic, environmental, and sociopolitical ramifications of its continued mass usage by both the industrial and developing world, we finally have the perfect storm for developing and improving alternatives to the petroleum fueled combustion engine.

Molecular hydrogen has the potential for serving as an alternative fuel for internal combustion engines. Its high energy-mass density (~55,000 Btu/lb), capability for near zero CO_2 and HC emissions in addition to the fact that it can be used as a renewable energy storage (for example, producing H_2 via water electrolysis using solar energy) puts it high on the list of alternative energy storage methods. It does however, have drawbacks such as energy-volume density that is an order of magnitude lower than gasoline (~76,000 Btu/ft^3 at 5000 psi) [1] which makes storage as a gas somewhat of a challenge for long range travel. Hydrogen exhibits several characteristics that can be

advantageous in this application including wide flammability range which allows ultra lean air-fuel ratios, quick flame propagation, and low ignition energy requirement.

These characteristics of hydrogen gas offer opportunities for improvement for use in internal combustion engines. Typical modern gasoline engines utilize computer controlled port fuel injection to deliver fuel to the engine. While this scheme works well for liquid hydrocarbon fuels, there are drawbacks to this method using hydrogen as a fuel. The low ignition energy requirement and fast flame propagation of hydrogen increase the probability of backfire through the engine's intake. Gaseous port injection also decreases the volumetric efficiency of the engine by displacing the available volume for air intake. Both issues can be improved by implementing direct injection of hydrogen into the cylinder, rather than through the intake manifold.

CHAPTER 2

LITERATURE REVIEW

Numerous articles have been written on the subject of hydrogen internal combustion engines, HICE, many dealing with optimizing the combustion process by maximizing engine efficiency, power output and minimizing emissions and unwanted backfires. A small summary of various journal articles that were helpful to our research and understanding the HICE process follows.

Sierens and Verhelst [2] took part in converting a big block V8 GM engine to run on hydrogen using a multiport sequential injection system. As stated above, ignition timing was optimized to maximize torque and minimize NOx emissions. The ignition timing required for mean best torque (MBT) was mainly dependent on the air fuel ratio and is dictated by the engine load, which is observed by changes in manifold absolute pressure (MAP). High load, high equivalence ratios (phi, Φ) required less timing (20° before top dead center, BTDC) while low load, low Φ required more (50° BTDC). It was noted that due to the high flame speed of hydrogen one would intuitively think that the range of ignition timings would be relatively narrow, however, due to the wide range of air fuel ratios (Φ = 0.2 - 0.5) this is not the case.

Injection duration and timing was optimized as well. Duration varies widely across the rpm range; at 750 rpm 3 ms of fuel is required equaling 13.5° of angular duration while at 3750 rpm under high load durations up to 14 ms are required equaling 315° of crank duration. This is the physical upper limit due to the fact that the inlet valve is open for 317° crank duration. Timing of the injection was found to be greatly important as well and has a strong influence on engine efficiency especially at low engine speed. This

parameter was responsible for changes in power output up to 20% and should start later at idle and increase as rpm increases.

Zhou et al. [3] reported on modeling and experimental testing of backfire prediction using a multiport sequential injection 4 cylinder engine. It was noted that due to the low required ignition energy of hydrogen the potential for knocking and backfire is increased mainly due to hot spots in the combustion chamber produced during the previous combustion cycle. Therefore, their main focus was predicting and testing the parameters which influence this phenomenon. Their modeling showed the tendency for hydrogen to backflow into the intake manifold prior to the intake valve closing if injection timing was early. The flow model simulation produced by the group proved to be a useful tool in predicting injection end timing as a function of engine speed and Φ, as their predictions showed good correlation to the general trends of experimental data.

Mohammadi et al. [4] performed a very thorough evaluation of an 858 cc single cylinder direct injection (DI) HICE converted from DI diesel engine. Testing consisted of varying hydrogen injection timing during the intake stroke (300° BTDC), early and late compression stroke (130° and 100° BTDC). Equivalence ratios and ignition timing were varied at each injection timing and several parameters including brake thermal efficiency, brake mean effective pressure, and NOx were recorded. It was noted that with early injection (intake valve still open) in cylinder maximum mean effective pressure decreased compared to the original diesel engine, though interestingly, it increased with later injection (sealed cylinder) and exceeded that of the original diesel configuration. Brake thermal efficiency followed the same trend and exceeded 38.9%. It was also shown that the largest factor contributing to the production of NOx was richer air-fuel

mixtures, of which $\Phi = 0.5$ showed to be the upper limit to reasonable NOx production. The group concludes deducing that late injection during the compression stroke (after intake valve closure) increases thermal efficiency and maximum power output while reducing NOx production via lean operation.

Choi et al. [5] discuss the cause of combustion cycle coefficient of variation (COV) in HICEs and its effect on performance and stable engine operation. They note that the variation in combustion causes a change in the mean effective pressure observed in cylinder. Possible causes of this variation are differences in fuel-air flow at the time of ignition, heterogeneity of the mixture, and the mixture of fresh air and residual gases near the ignition source. This divides the theories into two groups; that overall variation is caused by variation in early combustion and/or that it is caused by the period of rapid combustion. The group uses a 433 cc single cylinder engine with direct injection occurring during the early period of the compression stroke. They tested the effect of engine speed, injection timing, air-fuel ratio and spark timing on the coefficient of cycle variation. Combustion was stable across the range of rpm tested (1200-1800 rpm) although COV gradually increases. Injection timing optimally coincides with intake valve closure and COV rapidly increases as crank angle approaches top dead center, TDC. Engine operation was stable across a wide range of air fuel ratio, AFR ($0.6 < \Phi < 1.4$). Finally, operation is stable near MBT ignition timing and similar to injection timing, COV increases abruptly with timing approaching TDC.

CHAPTER 3

SPARK PLUG/INJECTOR FIRST DESIGN

Project Background

The following thesis describes ongoing research conducted by the UNLV Center for Energy Research (CER) in partnership with the Las Vegas Valley Water District (LVVWD). A great deal of work had been completed by previous graduate students Ronald Fifield, Julian Gardner and Evangeline Bulla [6-8] prior to the work described here.

The first phase of their work includes the conversion of a Polaris Ranger all terrain vehicle (ATV) from a carbureted, gasoline fueled engine to computer controlled hydrogen direct injection. Several of the components required for the conversion were designed, fabricated and tested by these students. This conversion utilized a cylinder head that had been modified for a pathway allowing injection of hydrogen directly into the cylinder rather than through more typical manifold port injection. An aftermarket fuel injection controller is utilized to actuate a commercially available, high pressure, hydrogen gas compatible solenoid to regulate hydrogen flow to the engine. A special check valve designed and fabricated by Ron Fifield [6] is incorporated between the solenoid and cylinder head in order to protect the solenoid from the extreme pressures and temperatures associated with the combustion process.

Figure 1. Polaris engine with direct injection hydrogen fueling. Figure courtesy of R. Fifield [6].

The second phase of work involved the conversion of a Ford F-250 pickup which originally was configured to be fueled with compressed natural gas (CNG). One of the major goals of this project was to design a way to convert the engine to hydrogen direct injection without having to make any internal engine modifications, i.e., requiring no removal or machining of the cylinder heads. With this goal in mind a spark plug/injector assembly was designed which replaces the conventional spark plug with an assembly that provides a path for hydrogen to be injected in-cylinder as well as providing the spark ignition necessary for combustion initiation (Figures 2 & 3). This design also incorporates the check valve assembly required for protection of the hydrogen solenoid.

At the start of work discussed in this thesis, much of the effort required to convert the vehicle's fuel system from CNG to hydrogen had been completed [7]. Remaining tasks included integration of add-on electronics with the stock electrical system, installation and evaluation of the new spark plug/injector assemblies, tuning of the vehicles powertrain control module (PCM) and characterization of engine power output and emissions.

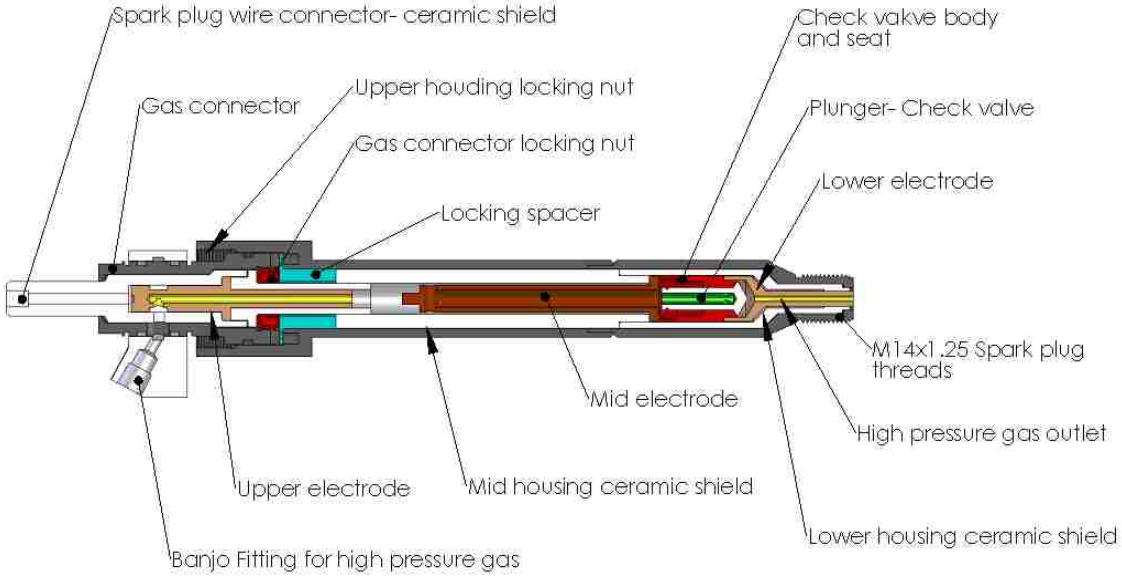

Figure 2. Hydrogen direct injection spark plug/injector assembly. Figure courtesy of R. Fifield [6].

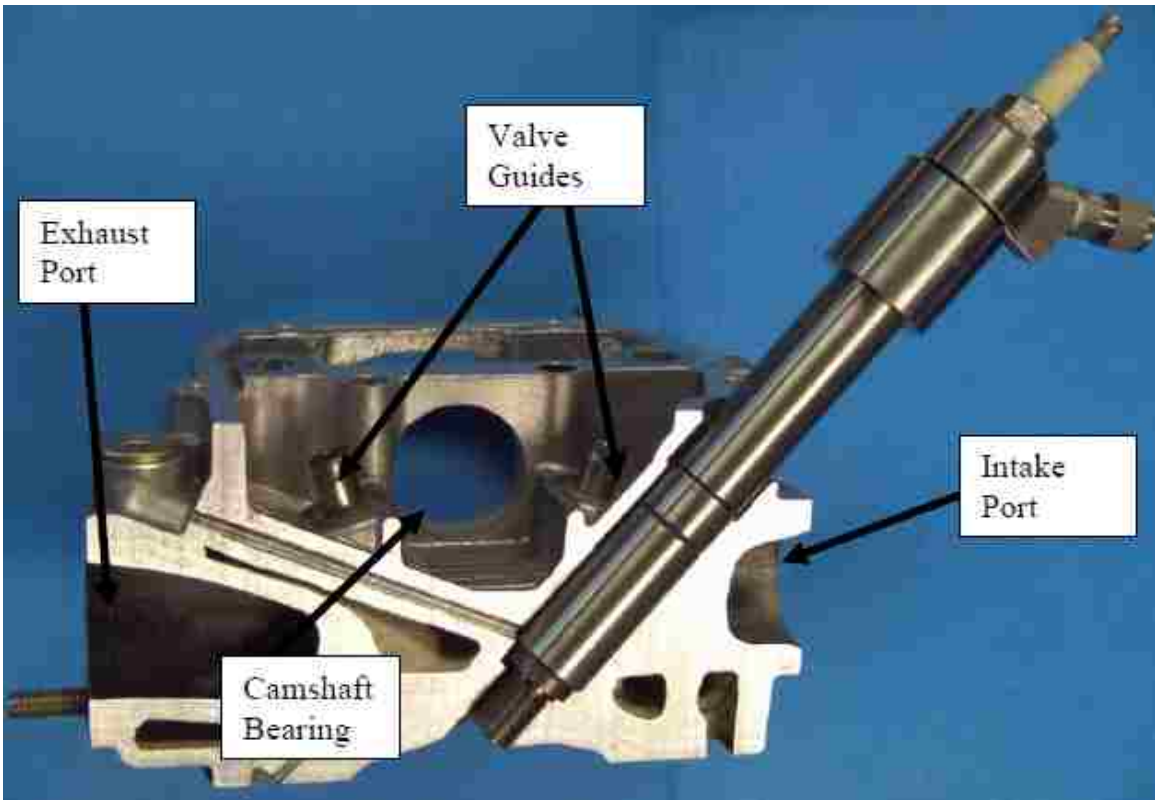

Figure 3. Polaris cylinder head cutaway displaying hydrogen direct injection spark plug/injector assembly. Figure courtesy of R. Fifield [6].

Hydrogen Conversion Electronics

Conversion of the Ford truck from natural gas (or gasoline) to hydrogen fueling requires several add-on electronic components which are available from various manufacturers. A short description of each is given here.

Pressure Transducer/Readout – An American Sensor Technologies 0-7000 psi pressure transducer is installed on the high pressure side of the hydrogen storage system and is used in conjunction with a Fuji FD500 Panel Meter which provides the in-cab readout. This assembly serves as a fuel level gauge for the hydrogen storage tanks.

Hydrogen Gas Sensors – Hydrogen leak detection sensors have been added to the vehicle under hood and in the bed of the truck. Alarm signal and current output occur at

10 and 20 percent of the lower flammability limit of hydrogen in air (corresponding to 4000 and 8000 ppm). The sensors have light emitting diode (LED) indicators as well as low current output used to trigger an in-cab alarm in the event of hydrogen leak.

Engine Hydrogen Solenoids / 12/24 V DC Step Up Converter – Eight Peter Paul high pressure solenoids are employed to control the flow of hydrogen to individual cylinders via the spark plug/injector assemblies. The solenoids are supplied with ~24V using a 12/24 V DC step up converter from Zahn Electronics. Increased voltage is used in order to decrease response time of the solenoids which are much larger than typical fuel injectors found in gasoline or natural gas fuel systems.

Peak and Hold Injector Driver – A peak and hold injector driver from Acceleronics adds additional circuitry necessary to run low impedance injectors/solenoids using the stock Ford PCM. Typical stock automotive PCMs are built to drive high impedance/low current injectors and are not capable of withstanding the increased current draw of larger low impedance injectors/solenoids. The injector driver is triggered by the Ford PCM injector circuits and controls eight separate injector drivers. The circuitry provides the peak and hold function which initially provides high current to the solenoid for decreased response times followed by a drop in current to hold the injector open, decreasing heat generation and power use by the circuit.

Wideband Oxygen Sensor – The PLX Devices wideband oxygen sensor is installed in the exhaust system and provides measurement of the engine operational air fuel ratio. Typical stock exhaust oxygen sensors only read a narrow range outside of stoichiometric AFR. The PLX wideband will allow tuning for AFR between 0.68 - 1.36 lambda (23.34 -

46.69:1 AFR for hydrogen). The sensor control box provides a linear 0-5V output corresponding to the AFR reading which can be data logged for engine tuning purposes.

Master Solenoid – A Clark Cooper solenoid valve is employed to isolate the hydrogen fuel system from the engine when not operating.

Timer – An Altronix multi-function timer is used during engine shutdown to isolate the supply of hydrogen from the engine.

A schematic of the add-on electronics system is shown in Figures 4 and 5. Experience gained from the Polaris ATV HICE conversion is employed here to decrease the chance of hydrogen gas leakage through the engine solenoids when the engine is not operating. During normal engine operation the vehicle's ignition switch will activate relays 1-4 providing power to the add on electronics and vehicle's PCM. During the engine shutdown procedure, when the ignition switch is turned off the timer is activated and provides a +12V trigger to keep relays 2, 3 and 4 activated for up to 60 seconds while allowing relay 1 (which is only activated by the vehicle's ignition switch) to be turned off. This closes the hydrogen supply master solenoid while continuing to provide power to the vehicle's PCM and the remainder of the add-on electronics. The engine will continue to run for up to 60 seconds after the master solenoid has been closed, evacuating the pressurized hydrogen fuel lines between the master solenoid and engine solenoids and preventing hydrogen gas leakage into the engine. This is done to decrease the probability of backfire when the engine is restarted.

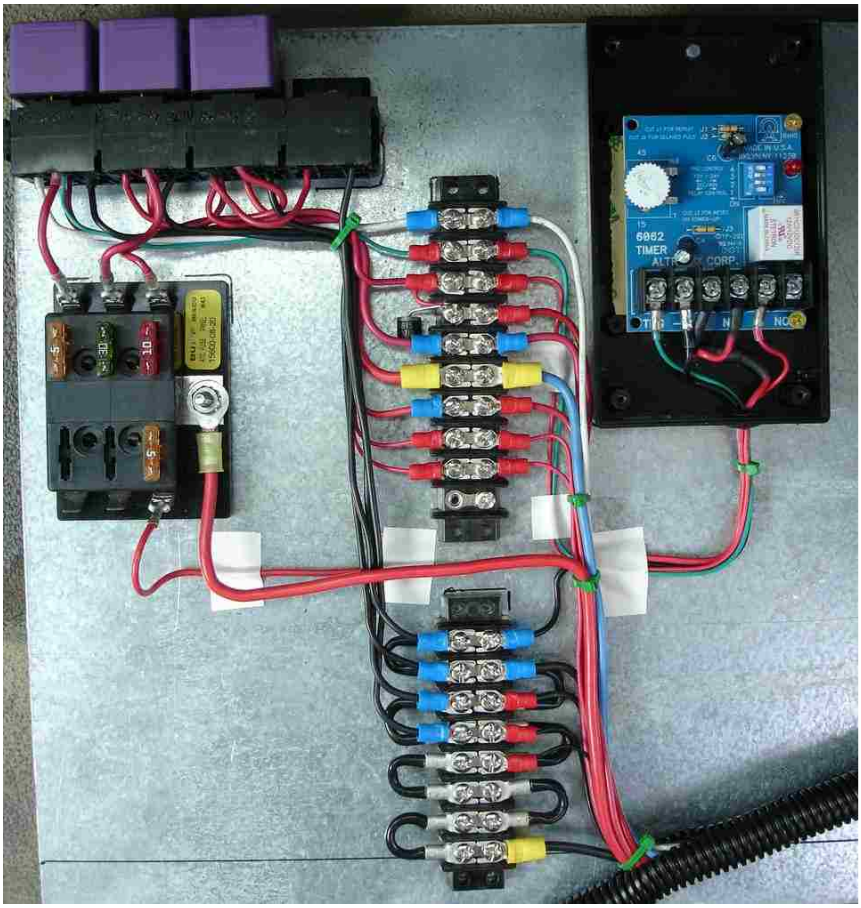

Figure 4. Modular wiring and electronics assembly

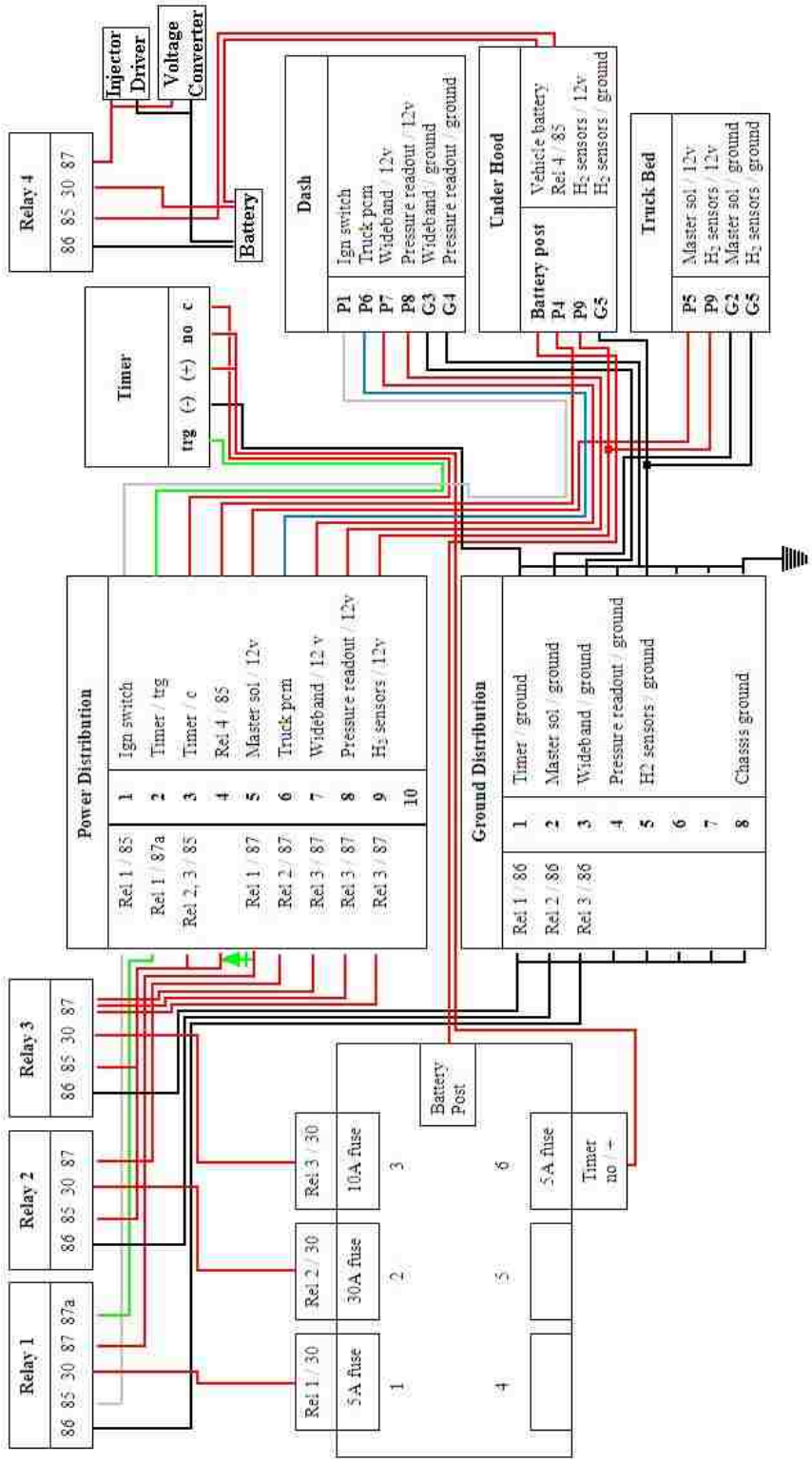

Figure 5. Hydrogen conversion add-on electronics schematic.

With the fuel and electronics systems in place, using software produced by SCT, a modified program was flashed into the vehicle's PCM that would allow the vehicle to run on hydrogen rather than natural gas. With these changes the engine was able to be started and run on hydrogen for the first time. The engine ran fairly well though the air fuel ratio was somewhat lean during operation. Figure 6 below shows a typical readout on a four channel oscilloscope monitoring the vehicle's crank sensor, cam sensor, and fuel injection and ignition signals. At this point the injectors are firing with the stock crank timing values; these values will be changed to occur during the compression stroke to decrease the probability of backfire during operation. Use of the oscilloscope allows verification of changes made to the vehicle's engine control module.

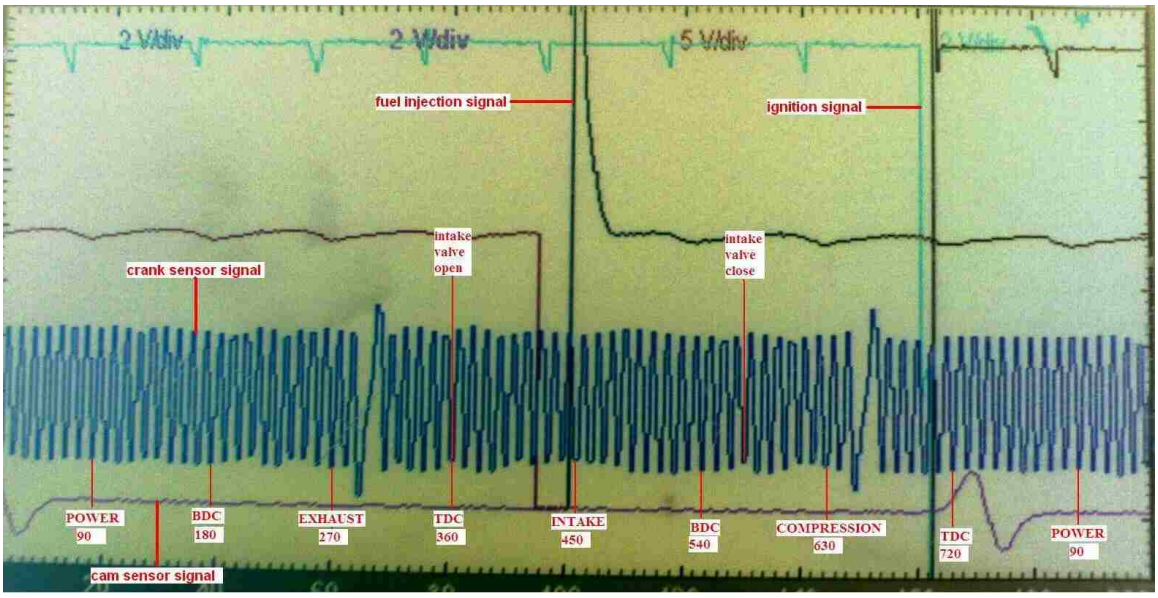

Figure 6. Four channel oscilloscope readout monitoring crank sensor, cam sensor, injector and ignition signals.

The day following initial startup, the engine developed a consistent exhaust backfire during operation. This was traced to two of the injector/spark plug assemblies that developed discontinuity through the electrode, inhibiting ignition of the air/fuel mixture. Hydrogen would pass through the cylinder to the exhaust where it would accumulate and ignite resulting in the observed backfire. Upon disassembly of the injectors it was noted that errors in machining tolerances allowed part of the electrode assembly to separate during operation resulting in loss of spark at the electrode tip. This was corrected by adjusting the tolerances and reassembling the injectors.

It was at this same time that noise coming from either the engine's valvetrain or rotating assembly was first noted. Compression and cylinder leak-down testing was performed to rule out mechanical problems with the engine. The compression values and leak-down percentages were found to be within specification considering that the engine in use has more than 136,000 miles of usage (Table 1).

Table 1. Results of cylinder compression and leak-down testing.

cylinder #	**1**	**2**	**3**	**4**	**5**	**6**	**7**	**8**
test 1 (psi)	111	110	100	111	109	112	108	115
test 2 (psi)	111	109	110	111	109	108	106	111
test 3 (psi)	107	112	110	114	111	108	105	110
average	109.7	110.3	106.7	112.0	109.7	109.3	106.3	112.0
leak down %	3	6	4	11	9	8	11	11

After repairs were made to the two problematic injectors previously mentioned, the engine operated fairly consistently for some time. The process of data logging (Figure 7) and altering the operating parameters of the PCM (Figure 8) to improve the consistency and performance of the engine then proceeded.

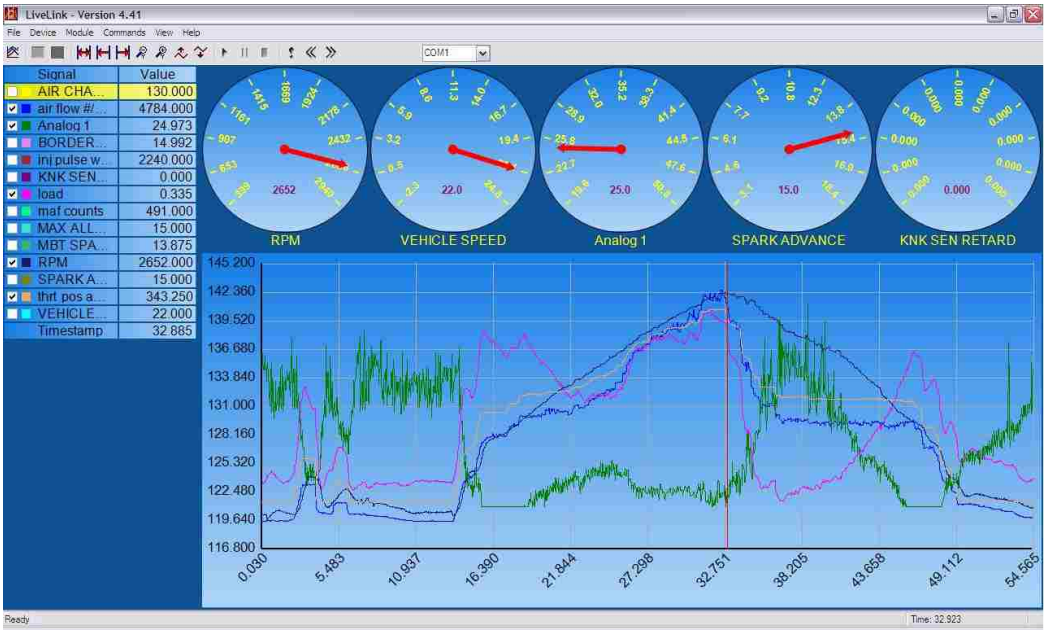

Figure 7. HICE Ford pickup data logging session using SCT LiveLink software.

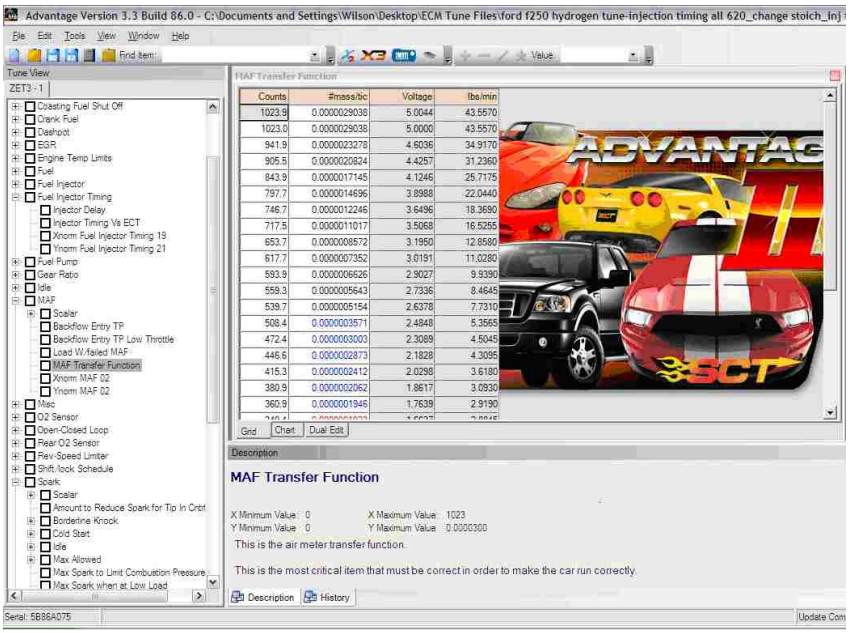

Figure 8. HICE Ford pickup powertrain control module programming using SCT Advantage III software.

After several data logging/tuning sessions another persistent backfire developed. The problematic injector/spark plug assembly was identified and removed from the engine for

testing. No issues with continuity were detected and resistance through the electrode assembly was measured to be 1.5 ohms (typical for the assembly). The spark function of the assembly was tested outside the engine using the vehicle's ignition system and appeared to be working, yet the backfire would return when the injector was reinstalled. The hypothesis that the injector was unable to ignite the hydrogen/air mixture in-cylinder during operation was verified by reinstalling the injector, running the engine, observing the backfire, then disconnecting the hydrogen solenoid supplying the same cylinder; when hydrogen was not supplied to the cylinder the backfire would cease to occur. This led to the following conclusion. With increased pressure in-cylinder, the spark would not jump the gap between the electrode and grounded housing resulting in hydrogen passing through the engine without being combusted and causing the exhaust backfire.

The injector was disassembled to find multiple cracks in the lower electrode ceramic insulator (Figure 9) which would easily allow spark to jump from the inner electrode to the injector's main housing rather than at the end of the injector.

Figure 9. Visible cracking of lower electrode ceramic insulator.

Spark Testing

With the loss of spark due to cylinder pressurization, the next step was to observe the spark function while under pressure. A pressure chamber with a viewing window was fabricated for this purpose and used in conjunction with a timing circuit (assembled by LVVWD technician, Richard Furniss) that would repeatedly trigger an ignition coil using a +12v power source. The injector with the broken lower ceramic was repaired by replacing the ceramic portion and reassembling. The first round of testing compared the repaired injector with an injector that was considered to be functioning properly (had no problems thus far). The testing arrangement is shown in Figure 10 below.

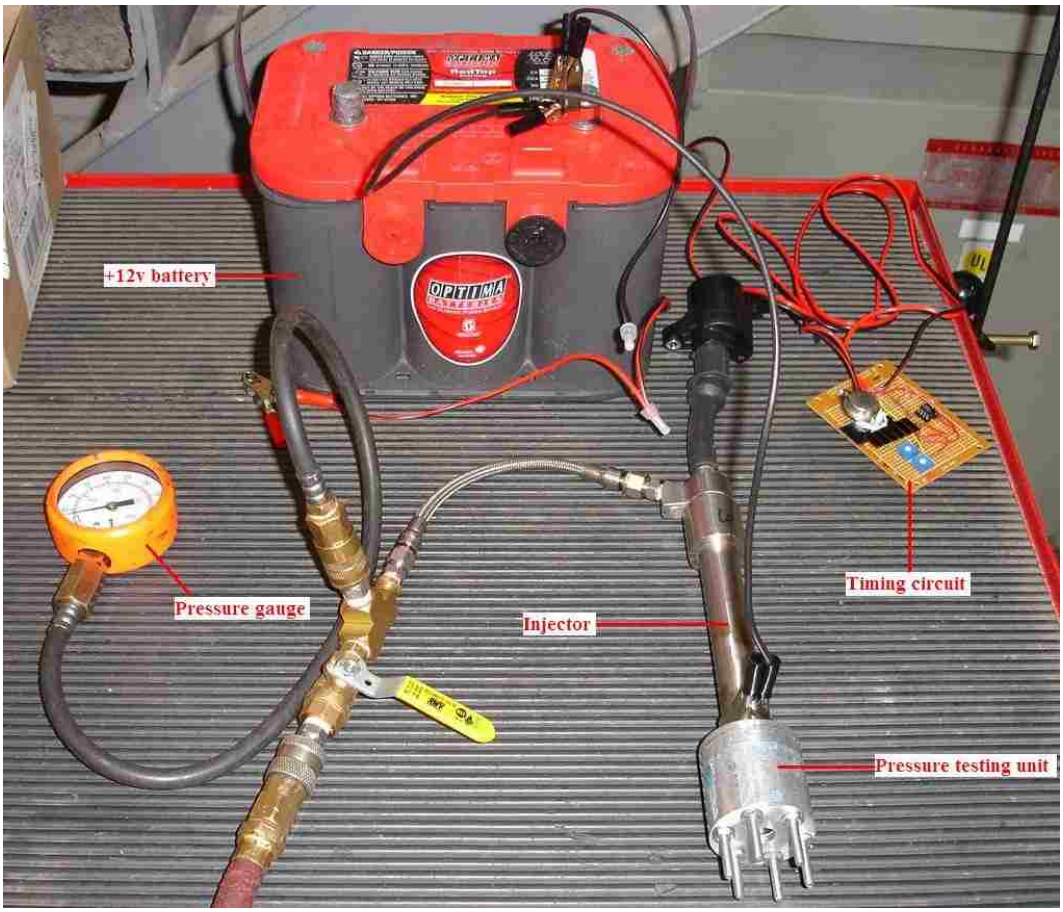

Figure 10. Pressurized spark testing apparatus.

Both were tested by observing the spark at zero psi and when pressurizing the chamber to ~110 psi. The good injector produced spark in both scenarios while the repaired injector produced spark but was erratic at both zero and high pressure. The problem injector was again disassembled and inspected; what looked to be a small fracture in the upper ceramic insulator was observed. The insulator was indeed cracked, allowing spark to ground to the injector housing. Although the crack is very minute, using the testing apparatus, spark can be seen jumping through the ceramic to a grounded probe as the resistance between the electrode and spark plug is increased by increasing the distance spark has to jump between the two. It was later determined after

disassembling the remainder of the injectors that the cracking in the ceramic pieces may be due to incorrect tolerances between the inner electrode and ceramic insulator. With insufficient tolerance between the two, it is likely that the combination of initial loading from assembly and heat cycling leading to expansion of the stainless steel electrode was sufficient to cause the ceramic insulator to fail during operation.

Another interesting observation was made during spark testing. While observing the spark performance with both the injector housing and pressure vessel pressurized, if the pressure within the injector housing is released, the electrode (in the still pressurized chamber) would cease arcing to the injector housing. In other words, when there is a great enough pressure differential between the injector housing and the end of the electrode, the resistance across the gap between the end of the electrode and the injector housing is too great for an arc to occur.

It is important to determine whether this can occur during normal engine operation. Using a direct injection scheme for hydrogen injection, the gas will inject during the compression cycle after the intake valve has closed. During injection, the hydrogen solenoid opens allowing hydrogen to flow through the injector and its internal check valve at a pressure of 400-800 psi. As this is happening the piston is traveling upward compressing the air/hydrogen mixture. The hydrogen will continue flowing until the solenoid is shut and the pressure differential across the check valve in the injector housing is equalized. After this point in-cylinder pressure will continue to increase as the piston approaches top-dead-center while pressure within the injector housing stays the same. The scenario may arise (depending on when hydrogen injection ends and how much ignition advance is commanded by the vehicle's engine control module) that if

cylinder pressure increases high enough above the pressure within the injector housing it is possible that the air/hydrogen mixture will not be ignited due to loss of spark across the electrode/housing gap.

The pressure testing apparatus was modified to allow pressurization of only the end of the housing to determine what pressure differential is required for spark to cease to occur. Prior to testing, each injector was disassembled and checked for evidence of cracks in the ceramic insulator; none were found with the exception of the previously mentioned damaged injector (injector #6 in the Table below). Each injector was tested by pressurizing the pressure chamber and observing the quality of the spark from the electrode to the grounded housing. The qualitative results of this testing is shown in Table 2 below.

Table 2. Testing of hydrogen injector spark quality at varying pressure.

test pressure (psi)	**injector #**							
	1	**2**	**3**	**4**	**5**	**6**	**7**	**8**
0	good	good	good	good	good	not tested	good	good
10	good	good	good	good	good	not tested	good	good
15	decreased	erratic	erratic	good	erratic	not tested	good	decreased
20	erratic	none	erratic	decreased	none	not tested	erratic	decreased
25	erratic	none	none	decreased	none	not tested	erratic	erratic
30	none	none	none	decreased	none	not tested	erratic	erratic
35	none	none	none	erractic	none	not tested	erratic	erratic
40	none	none	none	none	none	not tested	none	none
decreased spark performance at (psi)	**15**	**15**	**15**	**20**	**15**	**not tested**	**20**	**15**
failure at (psi)	**30**	**20**	**25**	**40**	**20**	**not tested**	**40**	**40**

Each injector displayed decreased spark performance at 20 psi or less and failed between 20-40 psi. To put this in perspective, cold cranking pressure for the Ford 5.4L engine was generally near 110 psi and can be expected to increase with an engine at

operational temperature and increased load/rpm. A conventional automotive spark plug was tested using the same apparatus as a control; spark was observed during pressurization from 0-100 psi using the same testing apparatus. In this case the spark intensity increased with increasing pressure and was most intense at the highest pressure. The results of this testing are of concern but it is worth noting the effects of the spark "blowout" due to the pressure differential across the hydrogen injector have not been directly observed during engine operation.

CHAPTER 4

SPARK PLUG/INJECTOR SECOND DESIGN

Component Design and Fabrication

A second spark plug/injector design has been produced that will attempt to solve the following list of potential problems with the current injectors:

- high cost (due to custom ceramic insulators and machining of stainless steel housing and electrode parts)
- cracking of ceramics due to varying tolerances, loading, vibration and heat cycling
- potential for leaks due to hydrogen gas having to flow through the electrode
- potential for spark failure due to pressure differential between combustion chamber and injector housing

A new design was modeled using Solid Works software, shown in Figures 11 and 12.

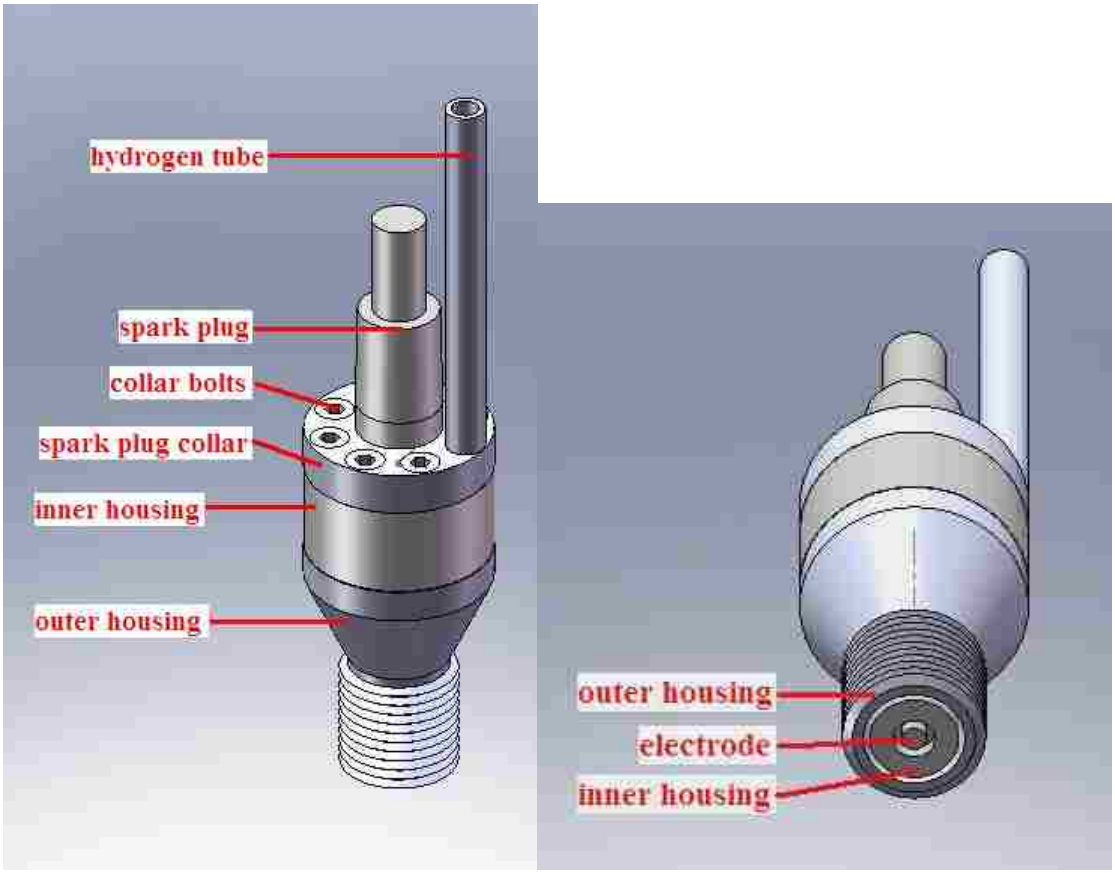

Figure 11. Second design hydrogen injector assembly.

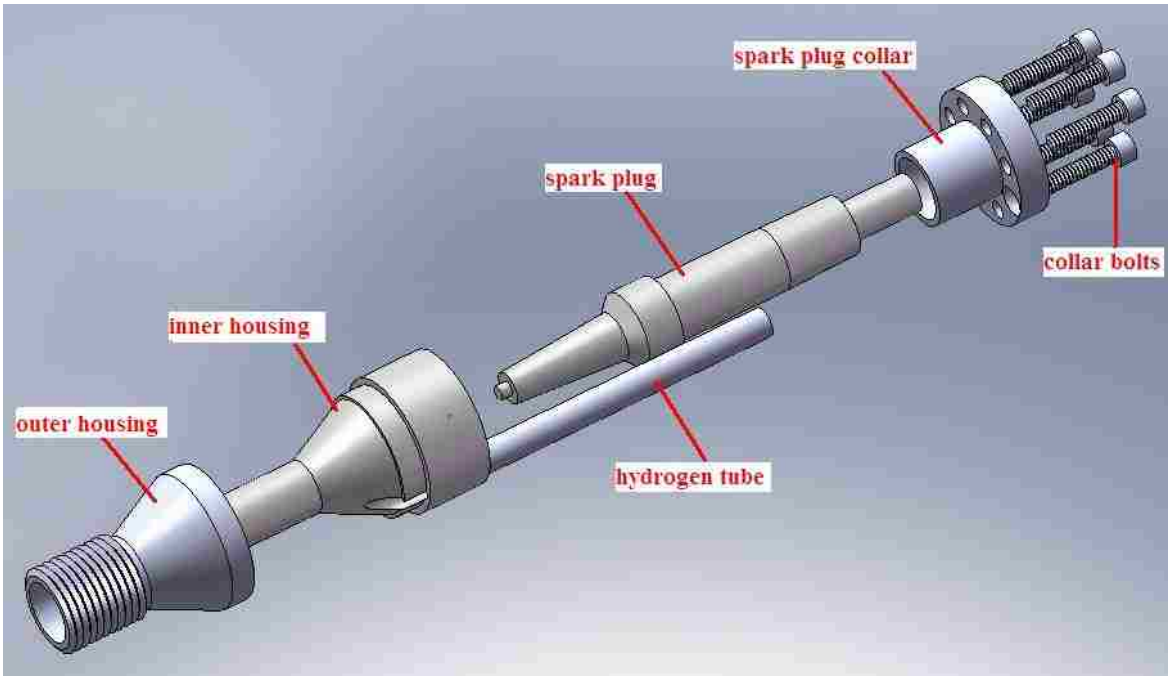

Figure 12. Second design hydrogen injector components, exploded view.

The assembly is simplified by separating the electrode/ceramic from the path for hydrogen gas (Figure 13). This greatly reduces the potential for spark failure by eliminating the pressure differential across the electrode in addition to eliminating gaps in the ceramic insulator. A conventional spark plug's ceramic and electrode assembly replaces the custom electrode and ceramic insulators, reducing cost of the assembly along with decreasing the probability of failure of expensive custom made parts. Prior to use, the outer metal housing for the spark plug must be separated from the inner ceramic and electrode to be used in the new injector (Figure 14).

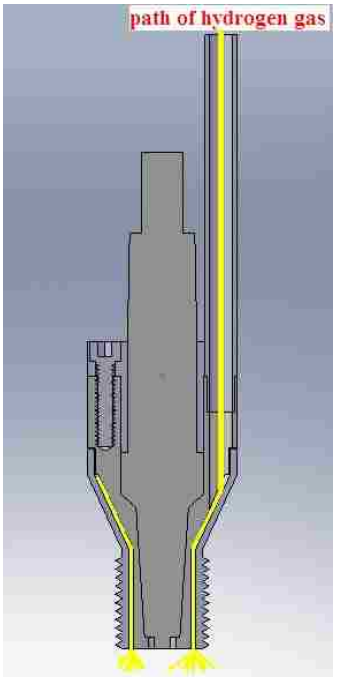

Figure 13. Path of hydrogen gas through injector.


Figure 14. Conventional spark plug disassembly.

The method of isolating the hydrogen solenoids from combustion heat/pressure using a check valve assembly developed by Ron Fifield [6] will still be used. It is contained in a separate housing outside the spark plug hole in the engine's cylinder head, due to space restrictions. A schematic of the check valve assembly and its integration with the hydrogen injector is shown in Figures 15 and 16.

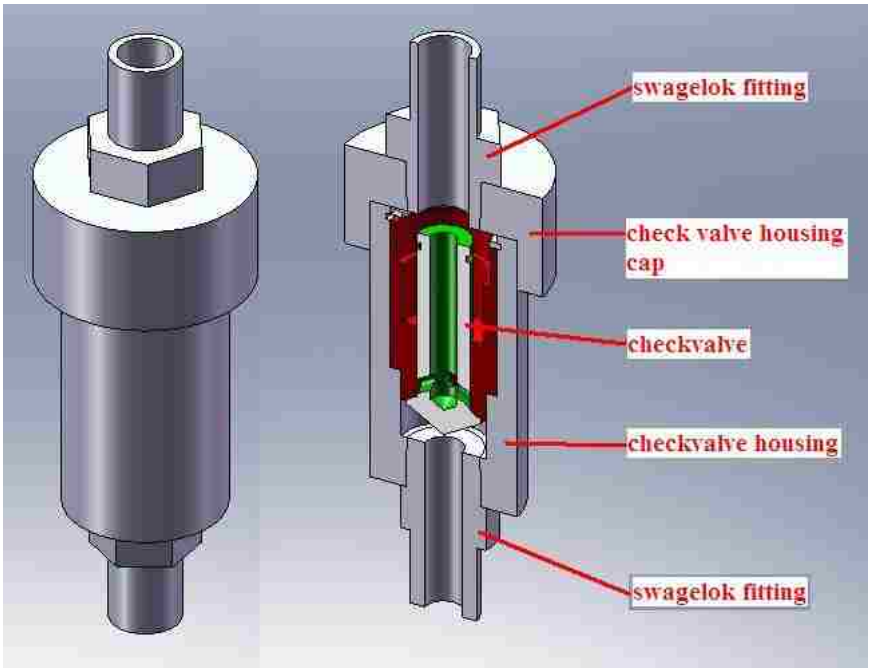

Figure 15. Check valve housing assembly cross-section.

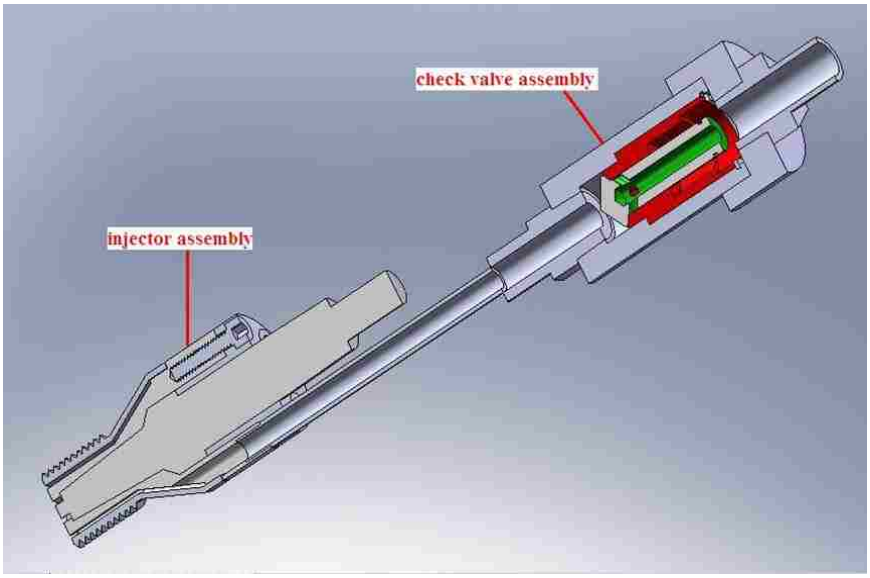

Figure 16. Injector and check valve assemblies.

Components for one complete injector assembly were first machined out of 6061 aluminum stock in order to determine the most efficient method of manufacture using the tools available in the UNLV Engineering Department machine shop (Figure 17). The machining process is simple enough that the injector and check valve housing can be completely machined in-house using a manual lathe and mill thus reducing cost from outsourced manufacturing.

Figure 17. Prototype injector assembly.

A set of spark plug/injectors and check valve housings were then fabricated using 316 stainless steel rod stock. Stainless steel was chosen for its anti-corrosive properties, machinability, weldability and resistance to embrittlement due to hydrogen exposure. The spark plug/injectors are assembled by TIG welding the hydrogen inlet tube to the inner housing followed by welding the inner and outer housing together, creating a sealed flow path for the hydrogen gas. The spark plug is then sealed to the inner housing using copper RTV sealant and retained by the spark plug collar and is secured using three #6-32 stainless machine screws (Figure 18). The check valve assembly utilizes an inner snap ring to retain the check valve. Sealing is accomplished using a Viton o-ring which compresses between check valve housing and cap when screwed together (Figure 19). Swagelok tube adapters are used on both ends to connect to the injector hydrogen inlet tube and the line from the external solenoid.

Figure 18. Second design spark plug/injector test assembly.

Figure 19. Check valve housing test assembly.

Component Evaluation

Spark Testing

Prior to installation, the spark function of the second design spark plug/injector was evaluated. Testing was conducted using the same apparatus as with the previous design and conducted using the same procedure; increasing air pressure within the pressure chamber at the electrode end and qualitatively observing the spark quality. Each assembly functioned as expected and in similar fashion to the control spark plug used. In this round of testing air pressure was increased sequentially up to 150 psi and with each increase more intense arcing was observed.

Injector Testing

In order to properly tune an electronically controlled fuel injected engine it is important to know various parameters with regards to the fueling system, including injector flow rates and response times. Characterization of these parameters for the solenoids and injector assemblies being used required assembling a testing apparatus that could drive the solenoids as if installed on the vehicle, obtain data during the process and collect and measure the hydrogen flow through the injector assemblies. This was done primarily using commercially available hardware and electronics. A General Motors engine control module (ECM) in conjunction with EFILive aftermarket control software is used to drive the solenoids and collect data from pressure and temperature sensors. Injector solenoid operation frequency is altered using a square wave function generator to provide the RPM signal to the GM ECM. Power is supplied to the solenoids using the Zahn Electronics 12/24V step-up converter and the peak and hold driving function

required for low impedance solenoids is provided by the Acceleronics injector driver. A schematic representation of the setup is shown in Figure 20.

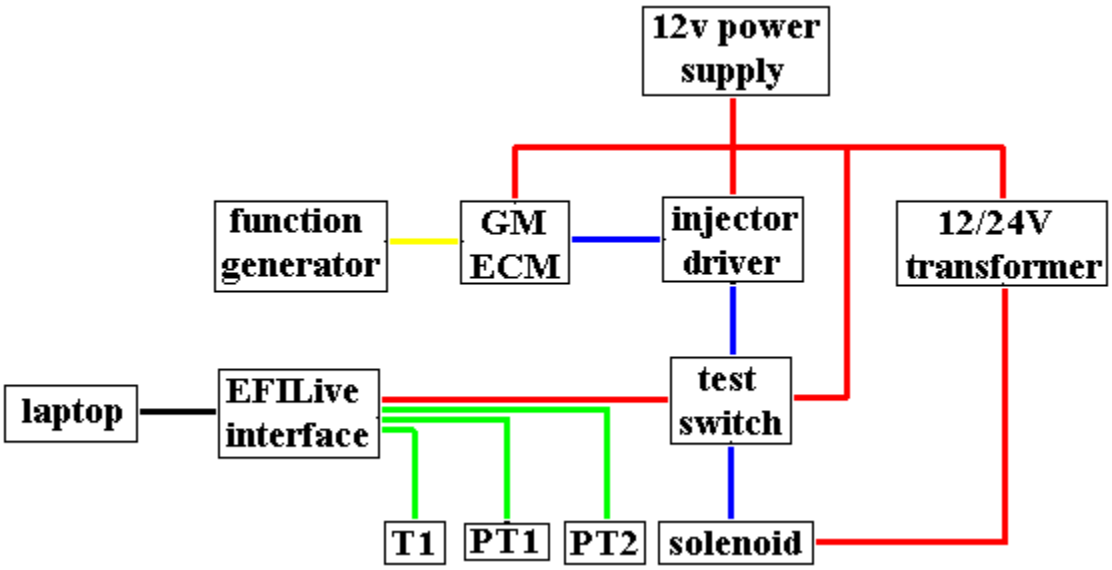

Figure 20. Schematic representation of injector testing electronics. PT1 = 0-7000 psi pressure transducer, PT2 = 0-500 psi pressure transducer, T1 = temperature sensor.

Solenoid Response Time

Solenoid response time is defined as the amount of time necessary for the solenoid to physically open allowing fuel flow after the ECM signals the solenoid to open. It is a function of multiple variables including but not limited to: solenoid pintle mass, fuel pressure, driver circuitry (eg. saturated vs. peak-and-hold) and circuit voltage. This value must be known in order to accurately command injector turn on times. A schematic of the test apparatus used to determine this value is shown in Figure 21.

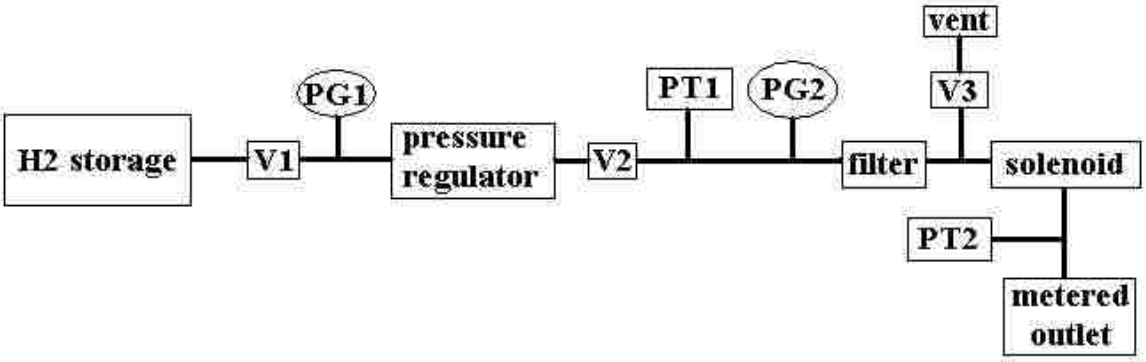

Figure 21. Schematic representation of solenoid response time testing apparatus. PG1 = 0-5000 psi analog pressure gauge, PG2 = 0-1000 psi analog pressure gauge, PT1 = 0-7000 psi pressure transducer, PT2 = 0-500 psi pressure transducer.

Solenoids were commanded to open for 65 ms at a frequency of 4.2 Hz (equivalent to a 4 stroke engine operating at 500 rpm) with a solenoid duty cycle of approximately 27 percent. Solenoid pulse width and pressure transducer voltages were observed using a Snap-On MODIS four channel oscilloscope. Response time is measured as the time required to reach 50% of the maximum pressure observed in similar fashion to testing conducted by Heffel et. al [9]. An example oscilloscope screen shot during testing is shown below in Figure 22; response time in this example is approximately 13 ms.

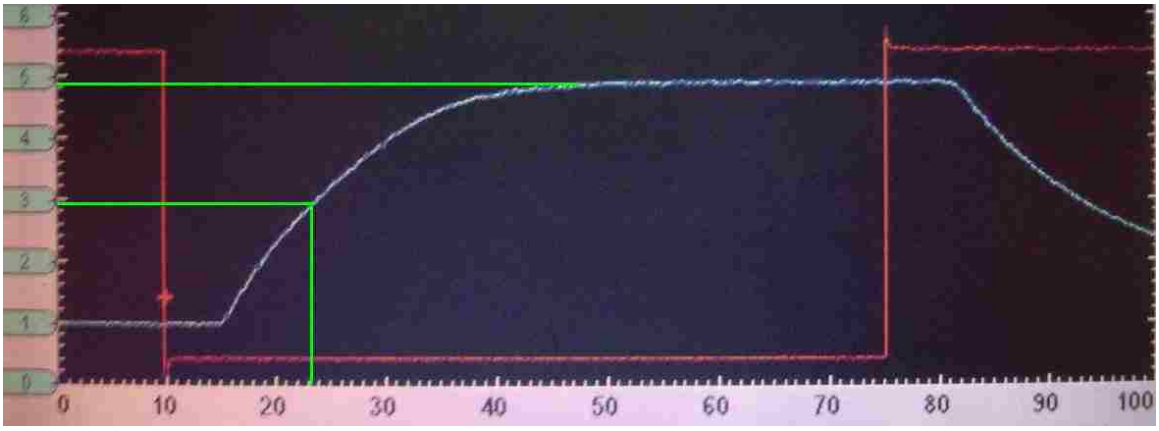

Figure 22. Example oscilloscope screen shot during testing. Response time in this example is approximately 13 ms. Red – solenoid commanded pulse width voltage, Blue – pressure transducer voltage, Green – response time measurement.

In order to observe both the effects of solenoid pressure and voltage testing was conducted at 400 and 600 psi with solenoid voltage at both 12 and 24.73V. Results are shown in Table 3.

Table 3. Solenoid response time testing results.

voltage	12	12		24.73	24.73
pressure (psi)	400	600		400	600
pulsewidth (ms)	65	65		65	65
response time (ms)	16	17		12	13

The observed response times are excessively slow, especially when compared to their gasoline direct injection counter parts which have opening times on the order of 0.4 ms [10].

Assembly Flow Testing

Flow testing was accomplished using a slightly modified version of the test apparatus used for solenoid response time testing. A schematic of the test apparatus is shown in Figure 23.

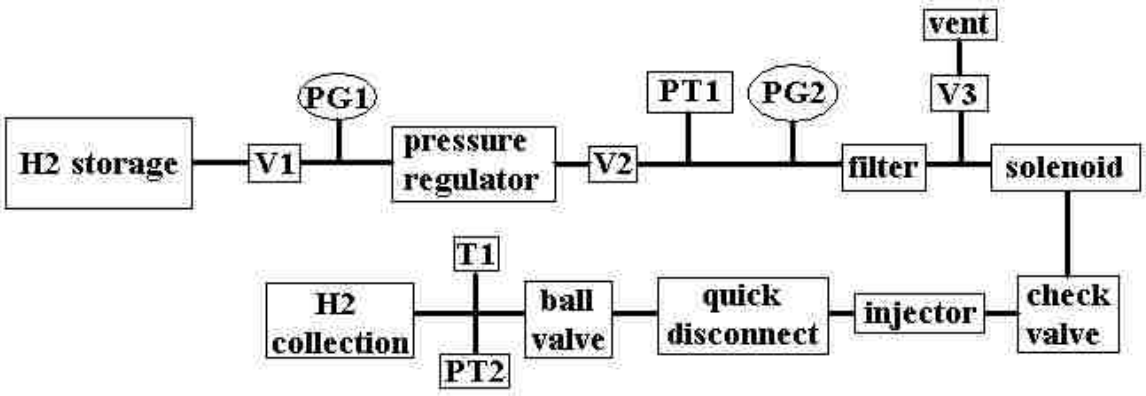

Figure 23. Schematic representation of injector flow testing apparatus. PG1 = 0-5000 psi analog pressure gauge, PG2 = 0-1000 psi analog pressure gauge, PT1 = 0-7000 psi pressure transducer, PT2 = 0-500 psi pressure transducer, T1 = temperature sensor.

In this scheme the hydrogen is injected for a known period of time through the check valve/sparkplug/injector setup (as it would be used on-vehicle) into a sealed plastic bag which can be isolated using a ball valve and separated from the test apparatus with a quick-disconnect pressurized gas fitting. The detached collection assembly is weighed before and after hydrogen collection with the difference representing the lift force generated by the buoyancy of the hydrogen gas. The lift force can then be used to calculate the amount of hydrogen gas present in the collection apparatus using the following expressions.

$$F_{lift} = W_{\underset{air}{displaced}} - W_{H_2} \tag{1}$$

$$F_{lift} = \rho_{\underset{air}{displaced}} * V_{\underset{air}{displaced}} - \rho_{H_2} * V_{H_2} \tag{2}$$

$$F_{lift} = \left(\rho_{\underset{air}{displaced}} - \rho_{H_2} \right) * V \tag{3}$$

$$F_{lift} = \left(\frac{\rho_{\underset{air}{displaced}}}{\rho_{H_2}} - 1 \right) * \rho_{H_2} * V \tag{4}$$

$$F_{lift} = \left(\frac{\rho_{\underset{air}{displaced}}}{\rho_{H_2}} - 1 \right) * W_{H_2} \tag{5}$$

$$W_{H_2} = \frac{F_{lift}}{\left(\frac{\rho_{displaced\ air}}{\rho_{H_2}} - 1 \right)} \tag{6}$$

With known values for the mass of hydrogen collected, duration of the test, solenoid operation frequency, pulse width and response time, the flow rate of the injector can be calculated.

$$\frac{\text{engine rpm}}{2} = \text{ solenoid frequency} \tag{7}$$

$$\text{solenoid frequency} * \text{total time of test} = \text{number of injection events} \tag{8}$$

$$\text{injector open time} = \text{commanded pulse width} - \text{response time} \tag{9}$$

$$\text{number of injection events} * \text{injector open time} = \text{total injector open time} \tag{10}$$

$$\frac{\text{H}_2 \text{ mass}}{\text{total injector open time}} = \text{injector flow rate} \tag{11}$$

Significant values for solenoid operation frequency and pulse width must be chosen prior to testing while taking into consideration the operational characteristics of in-cylinder fuel injection. In order to take advantage of the improvements in cylinder filling and volumetric efficiency that direct injection allows, fuel injection must occur in a

sealed cylinder during the compression stroke after the intake valve has closed. This greatly decreases the time available for injection when compared to intake manifold port injection. Typical camshaft profiles will close the intake valve several degrees after bottom dead center at the beginning of the compression stroke. The camshaft of the Ford 5.4L engine closes the intake valve at approximately 560 degrees referenced to TDC at the beginning of the power stroke (20 degrees into the compression stroke). This allows 160 degrees of crankshaft rotation for injection to take place, not considering the time required for ignition advance which will decrease the time available as well. The following relations can be used to convert from degrees of rotation available for injection to time available as a function of engine speed.

$$\left(\text{engine rpm} * \frac{360^\circ}{\text{rev}}\right)^{-1} = \frac{\text{time}}{\text{crankshaft degree}} \tag{12}$$

$$\frac{\text{time}}{\text{crankshaft degree}} * 160^\circ = \text{total time available for injection} \tag{13}$$

$$\left(\frac{\text{total time available for injection}}{\frac{\text{time}}{\text{crankshaft degree}} * 720^\circ}\right) * 100 = \text{solenoid duty cycle} \tag{14}$$

Calculations were carried out for the engine operating at 500, 2000, 3500 and 5000 rpm as shown in Table 4.

Table 4. Calculation of significant values for injector flow testing.

crankshaft degrees of rotation available for injection	160			
engine speed (rev/min)	500	2000	3500	5000
time/crankshaft degree (ms/deg)	0.3333	0.0833	0.0476	0.0333
total time available for injection (ms)	53.3	13.3	7.6	5.3
duty cycle (%)	22.2	22.2	22.2	22.2

Part of the strategy for this round of tests was to operate the solenoids near the maximum available time for injection for each rpm to be tested. With information gathered from solenoid response time testing, the decision was made to add 12 ms to each injector pulse width to allow time for injector opening. During flow testing it was observed that the solenoid operated erratically when the total commanded pulse width was greater than ~15.1 ms at 41.7 Hz (equivalent to engine speed of 5000 rpm). To remedy this problem, the total commanded pulse width was decreased to 15.1 ms, resulting in a lower duty cycle (12.8%) compared to the other tests which were run near 22% duty cycle. Frequency and pulse width operating parameters are shown in Table 5.

Table 5. Table of values used during injector flow testing.

engine speed (rev/min)	**500**	**2000**	**3500**	**5000**
injector operation frequency (Hz)	4.2	16.7	29.2	41.7
total time available for injection (ms)	53.3	13.3	7.6	5.3
actual pulsewidth tested (ms)	65.3	25.1	20.1	15.1
actual pulsewidth tested - 12 ms response time (ms)	53.3	13.1	8.1	3.1
duty cycle (%)	22.2	21.8	23.6	12.8

For this series of tests the solenoids were operated at 4.2, 16.7, 29.2 and 41.7 Hz, the equivalent of a 4 stroke engine operating at 500, 2000, 3500 and 5000 rpm. Flow rate was observed at varying pressures of 200, 400, 600 and 800 psi for each operation

frequency for a total of 16 tests. Four separate runs were conducted for each test. The average flow rate and standard deviation were calculated for each set of four runs. Testing results are shown in Table 6.

Table 6. Injector flow testing results.

		injector flow rate (lb/hr)						
		test number				average flow rate (lb/hr)	std dev	% std dev
rpm	psi	1	2	3	4			
500	200	4.32	4.32	4.32	4.34	4.32	0.01	0.26
500	400	10.59	10.43	10.20	10.40	10.41	0.16	1.54
500	600	16.94	16.91	16.66	16.66	16.79	0.15	0.91
500	800	23.29	22.84	22.51	23.03	22.92	0.33	1.43
2000	200	5.90	6.97	6.03	6.02	6.23	0.49	7.93
2000	400	16.65	16.26	16.65	16.48	16.51	0.18	1.12
2000	600	26.49	26.21	26.96	25.90	26.39	0.45	1.71
2000	800	36.22	35.75	35.33	35.91	35.80	0.37	1.04
3500	200	9.49	9.53	9.35	9.43	9.45	0.08	0.82
3500	400	22.44	22.45	22.35	22.35	22.40	0.05	0.24
3500	600	33.75	35.95	33.44	34.20	34.34	1.12	3.26
3500	800	46.17	47.14	46.81	47.44	46.89	0.54	1.16
5000	200	18.54	18.70	18.36	18.63	18.56	0.15	0.79
5000	400	44.98	45.56	45.74	45.72	45.50	0.36	0.78
5000	600	70.09	70.48	72.39	70.59	70.89	1.03	1.45
5000	800	100.93	91.50	90.72	97.96	95.28	4.97	5.22

Plots of injector flow rate data vs. hydrogen pressure and solenoid pulse width are shown in Figures 24 & 25.

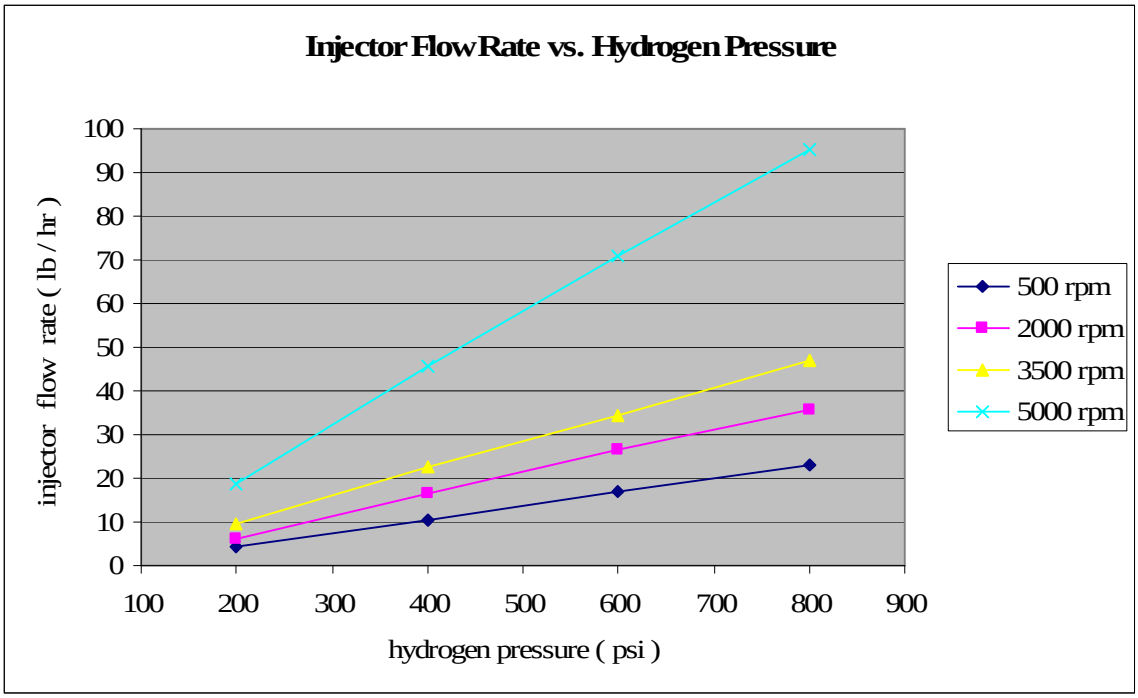

Figure 24. Injector flow rate vs. hydrogen line pressure.

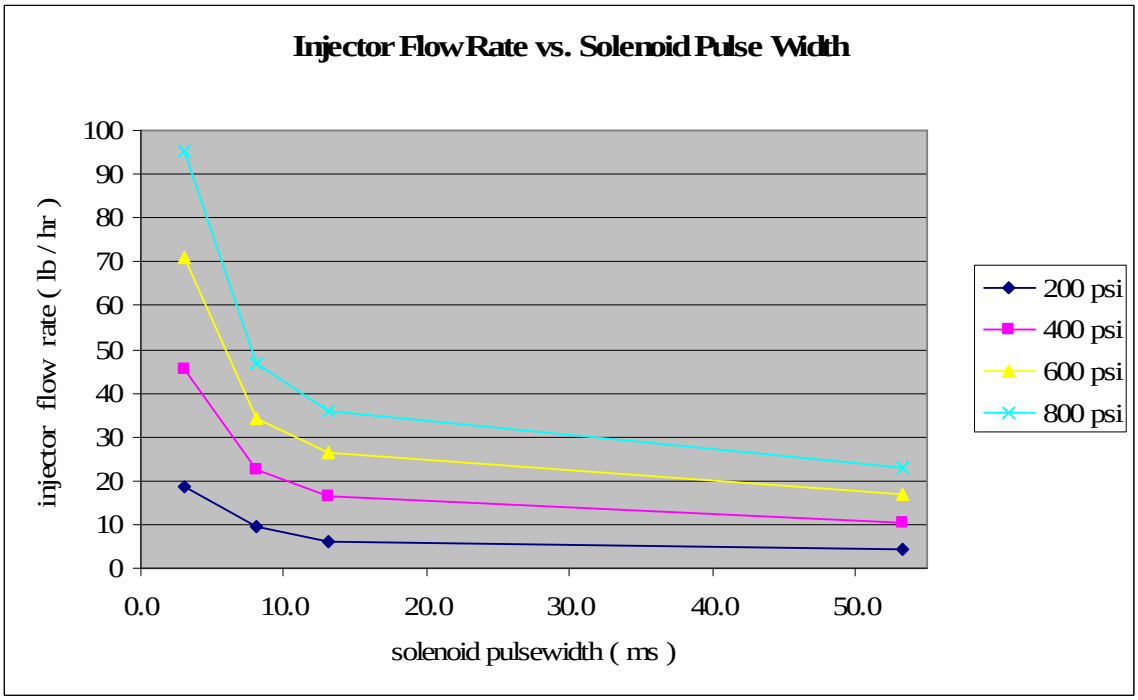

Figure 25. Injector flow rate vs. solenoid pulse width.

It is evident from the graphs that the flow rate increases in a linear fashion with increase in pressure for each solenoid frequency (rpm) tested. One result that was not expected was the nonlinear increase in flow rate at low pulse width/high frequency solenoid operation.

Injector flow rate data can now be used to determine whether the injectors can meet the fueling requirements of the engine. Based on the engine displacement and stoichiometric air fuel ratio for hydrogen gas (34.33:1), the mass of hydrogen required per injection event can be calculated.

$$\text{engine displacement} = 5.4\text{L} / 330\ \text{in}^3 \tag{15}$$

$$\text{cylinder volume} = 41.25\ \text{in}^3 \tag{16}$$

$$\text{cylinder volume} * \text{air density} = \frac{\text{mass air}}{\text{cyl}} \tag{17}$$

$$\frac{\text{mass air} \,/\, \text{cyl}}{\text{afr}} = \frac{\text{mass } H_2}{\text{cyl}} = \text{mass } H_2 \text{ required per injection} \tag{18}$$

Using the total time available for injection (eqn. 13) and the injector flow rate, the mass of hydrogen per injection is calculated.

$$\text{total time available for injection} * \text{injector flow rate} = \frac{\text{mass } H_2}{\text{injection}} \tag{19}$$

The percent of required hydrogen delivery achieved per injection event is calculated as,

$$\frac{\text{mass } H_2 \text{ / injection}}{\text{mass } H_2 \text{ required per injection}} * 100 = \%\text{ of required } H_2 \text{ delivery achieved} \qquad (20)$$

Results of these calculations are shown in Table 7. Yellow highlighting represents values that did not achieve the required hydrogen gas delivery while values highlighted in green achieve sufficient fuel delivery.

Table 7. Calculation of percent of required H_2 delivered.

engine speed (rpm)	500	500	500	500
hydrogen pressure (psi)	200	400	600	800
average flow rate (lb/hr)	4.32	10.41	16.79	22.92
% of required H2 delivery achieved	114.3	275.1	443.9	605.8

engine speed (rpm)	2000	2000	2000	2000
hydrogen pressure (psi)	200	400	600	800
average flow rate (lb/hr)	6.23	16.51	26.39	35.80
% of required H2 delivery achieved	41.2	109.1	174.4	236.6

engine speed (rpm)	3500	3500	3500	3500
hydrogen pressure (psi)	200	400	600	800
average flow rate (lb/hr)	9.45	22.40	34.34	46.89
% of required H2 delivery achieved	35.7	84.6	129.7	177.1

engine speed (rpm)	5000	5000	5000	5000
hydrogen pressure (psi)	200	400	600	800
average flow rate (lb/hr)	18.56	45.50	70.89	95.28
% of required H2 delivery achieved	49.1	120.3	187.4	251.9

Engine Testing

The next step in testing the spark plug/injector assemblies was to install them in the Ford engine and begin the process of tuning the vehicle's PCM (Figure 26). Upon startup, several exhaust backfires occurred which has been a typical occurrence for an untuned vehicle. Once the engine was running consistently, a significant knocking sound was detected coming from the lower end of the engine. The knock was traced to the number eight cylinder and is likely coming from the piston/rod assembly as opposed to the valvetrain. The engine was run in this way for at least 30 minutes without the situation improving. Compression and cylinder leak-down tests were performed; no obvious signs of damage were noted. At this point, nearing the end of the time allotted for the project, there unfortunately was not sufficient time available to remove and disassemble the engine to diagnose and repair the problem.

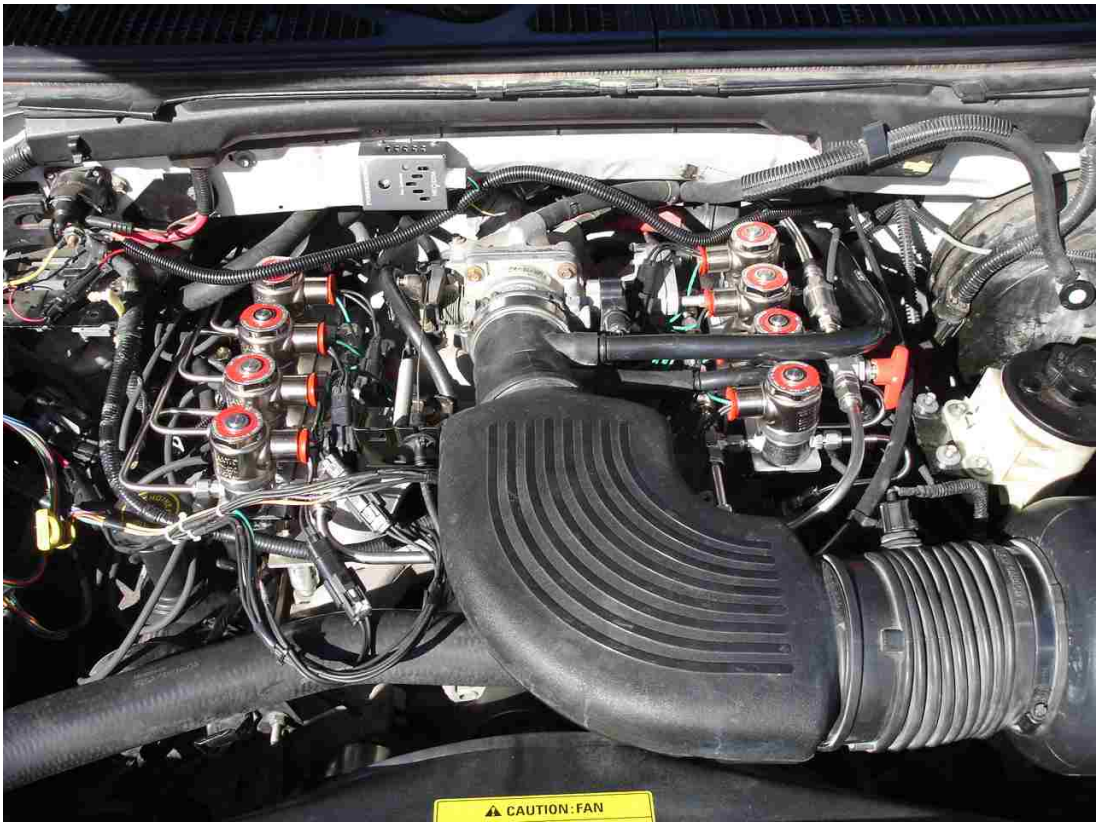

Figure 26. Completed installation of hydrogen direct injection system on Ford 5.4L engine.

CHAPTER 5

DISCUSSION AND CONCLUSIONS

Conversion of a hydrocarbon fueled internal combustion engine has been accomplished using hydrogen direct injection. The experience gained from conversion of a Polaris ATV has been applied to the Ford pickup discussed here. Rather than requiring disassembly and modification of the engine's cylinder head to provide a path for in-cylinder injection, a new component replaces the conventional spark plug and serves as both spark plug and injector, enabling conversion without internal engine modification. A second design spark plug/injector has been developed to improve issues encountered with first design. Problems with erratic spark function, ceramic failures, and manufacturing cost and complexity have been greatly reduced. Further testing of the assemblies is required to determine the reliability of function.

The hydrogen engine solenoids used on these projects have been tested to characterize response times and flow rates when used with the injector assemblies. The large mass of the solenoids is likely to cause the relatively long duration response times observed. This may become an issue for high rpm operation as the sum of the solenoid response, open and closing times approaches the time required to complete a full engine cycle, preventing the solenoid from fully opening or closing. Erratic behavior observed when the solenoids were commanded to open longer than 15.1 ms at 41.7 Hz may be a result of this slow function. Response is improved with the solenoids operating at higher voltage as can be seen with the 4 ms improvement from doubling the voltage from 12 to 24 V. Operation at even higher voltage would likely increase this improvement, though

upgrades to the injector driver electronics would be required to handle the additional power.

Characterization of the solenoid/injector flow rate has shown that adequate fueling is possible with hydrogen line pressure at 600-800 psi up to 3500 rpm. Flow was shown to increase linearly with increased pressure for the same frequency/pulse width operation. A nonlinear increase in flow rate was observed with a combination of increased injector frequency decreased pulse width. The large increase in flow rate at high frequency (41.7 Hz) and low pulse width (3.1 ms) operation may be due to the long response time previously mentioned. It is possible that the solenoid may not have sufficient time to actuate at high engine speed, resulting in a false flow rate reading. This phenomenon would impair accurate fueling and should be confirmed with additional testing.

BIBLIOGRAPHY

[1] "Module 3: Hydrogen use in internal combustion engines." College of the Desert, Dec. 2001. <http://www1.eere.energy.gov/hydrogenandfuelcells/tech_validation/pdfs/fcm03r0.pdf >

[2] Sierens R, Verhelst S. "Aspects concerning the optimization of a hydrogen fueled engine." Int J Hydrogen Energy 2007; 32 (1): 296-304.

[3] Liu X, Liu F, Zhou L, Sun B, Schock HJ. "Backfire prediction in a manifold injection hydrogen internal combustion engine." Int J Hydrogen Energy 2008; 1-9.

[4] Mohammadi A, Shioji M, Nakai Y, Ishikura W, Tabo E. "Performance and combustion characteristics of a direct injection SI hydrogen engine." Int J Hydrogen Energy 2007; 32 (1): 296-304.

[5] Kim YY, Lee JT, Choi GH. "An investigation on the causes of cycle variation in direct injection hydrogen fueled engines." Int J Hydrogen Energy 2005; 30(1):69–76.

[6] Fifield, R. "Development of in-cylinder injection for a hydrogen internal combustion engine." Thesis, University of Nevada, Las Vegas. Dept. of Mechanical Engineering 2007.

[7] Gardner, J. "Conversion and performance evaluation of a hydrogen powered Ford F-250 pickup truck." Thesis, University of Nevada, Las Vegas. Dept. of Mechanical Engineering 2007.

[8] Bulla, E. "The design and testing of a hydrogen fueled internal combustion engine." Thesis, University of Nevada, Las Vegas. Dept. of Mechanical Engineering 2006.

[9] Heffel, JW, McClanahan, MN, Norbeck, JM. "Electronic fuel injection for hydrogen fueled internal combustion engines." SAE Technical Paper 1998; 981924: 1-11.

[10] "Delphi Multec GDi Multi-Hole Fuel Injectors." Delphi Corporation, 2009. <https://delphi.com/shared/pdf/ppd/pwrtrn/gas_multec_gdi_inj.pdf>

VITA

Graduate College
University of Nevada, Las Vegas

Maxwell A. Wilson

Degrees:
Bachelor of Science, Chemistry, 2002
University of Nevada, Las Vegas

Thesis Title: Development of Hydrogen Direct Injection for Conversion of Internal Combustion Engines.

Thesis Examination Committee:
Chairperson, Dr. Robert Boehm, Ph. D.
Committee Member, Dr. Yitung Chen, Ph. D.
Committee Member, Dr. Suresh Sadineni, Ph D.
Graduate Faculty Member, Dr. Yahia Baghzouz, Ph. D.